Biomedical Optics EXPRESS

Accurate position tracking of optically trapped live cells

Niall McAlinden,[1,*] David G. Glass,[1,2] Owain R. Millington,[2] and Amanda J. Wright[3]

[1] *Institute of Photonics, University of Strathclyde, Wolfson Centre, Glasgow, G4 0NW, UK*
[2] *Strathclyde Institute of Pharmacy and Biomedical Sciences Glasgow, G4 0RE, UK*
[3] *Institute of Biophysics, Imaging and Optical Science (IBIOS), Life Science Building, University of Nottingham, University Park, Nottingham, NG7 2RD, UK*

[*]*niall.mcalinden@strath.ac.uk*

Abstract: Optical trapping is a powerful tool in Life Science research and is becoming common place in many microscopy laboratories and facilities. There is a growing need to directly trap the cells of interest rather than introduce beads to the sample that can affect the fundamental biological functions of the sample and impact on the very properties the user wishes to observe and measure. However, instabilities while tracking large inhomogeneous objects, such as cells, can make tracking position, calibrating trap strength and making reliable measurements challenging. These instabilities often manifest themselves as cell roll or re-orientation and can occur as a result of viscous drag forces and thermal convection, as well as spontaneously due to Brownian forces. In this paper we discuss and mathematically model the cause of this roll and present several experimental approaches for tackling these issues, including using a novel beam profile consisting of three closely spaced traps and tracking a trapped object by analysing fluorescence images. The approaches presented here trap T cells which form part of the adaptive immune response system, but in principle can be applied to a wide range of samples where the size and inhomogeneous nature of the trapped object can hinder particle tracking experiments.

OCIS codes: (170.0180) Microscopy; (350.4855) Optical tweezers or optical manipulation; (180.2520) Fluorescence microscopy; (110.2960) Image analysis; (070.6120) Spatial light modulators.

References and links

1. J. E. Molloy and M. J. Padgett, "Lights, action: optical tweezers," Contemp. Phys. **43**(4), 241–258 (2002).
2. J. M. Tam, C. E. Castro, R. J. W. Heath, M. L. Cardenas, R. J. Xavier, M. J. Lang, and J. M. Vyas, "Control and Manipulation of Pathogens with an Optical Trap for Live Cell Imaging of Intercellular Interactions," PLoS ONE **5**(2), 15215 (2010).
3. Y. Su and L. Hsu, "Measurement of Macrophage Adhesion at Various pH Values by Optical Tweezers with Backward-Scattered Detection," Jpn. J. Appl. Phys. **49**, 077002 (2010).
4. X. Wei, M. Si, D. K. Imagawa, P. Ji, B. J. Tromberg, and M. D. Cahalan, "Perillyl Alcohol Inhibits TCR-Mediated $[Ca^{2+}]_i$ Signaling, Alters Cell Shape and Motility, and Induces Apoptosis in T Lymphocytes," Cell. Immunol. **201**, 6–13 (2000).
5. B. Anvari, J. H. Torres, and B. W. McIntyre, "Regulation of pseudopodia localization in lymphocytes through application of mechanical forces by optical tweezers," J. Biomed. Opt. **9**(5), 865–872 (2004).
6. P. A. Negulescu, T. B. Krasieva, A. Khan, H. H. Kerschbaum, and M. D. Cahalan, "Polarity of T Cell Shape, Motility, and Sensitivity to Antigen," Immunity **4**, 421–430 (1996).

#200917 - $15.00 USD Received 20 Nov 2013; revised 20 Dec 2013; accepted 20 Dec 2013; published 3 Mar 2014

7. X. Wei, B. J. Tromberg, and M. D. Cahalan, "Mapping the sensitivity of T cells with an optical trap: Polarity and minimal number of receptors for Ca^{2+} signaling," Proc. Natl. Acad. Sci. USA **96**, 8471–8476, (1999).
8. K. Neuman and S. Block, "Optical trapping," Rev. Sci. Instrum. **75**(9), 2787–27809 (2004).
9. S. Keen, J. Leach, G. Gibson, and M. J. Padgett, "Comparison of a high-speed camera and a quadrant detector for measuring displacements in optical tweezers," J. Opt. A: Pure Appl. Opt. **9**, S264–S266 (2007).
10. M. Andersson, A. Madgavkar, M. Stjerndahl, Y. Wu, W. Tan, and R. Duran, "Using optical tweezers for measuring the interaction forces between human bone cells and implant surfaces: System design and force calibration," Rev. Sci. Instrum. **78**, 074302 (2007).
11. S. Oddos, C. Dunsby, M. A. Purbhoo, A. Chauveau, D. M. Owen, M. A. A. Neil, D. M. Davis, and P. M. W. French, "High-Speed High-Resolution Imaging of Intercellular Immune Synapses Using Optical Tweezers," Biophys. J: Biophys. Lett. **96**(10), L66–L68 (2008).
12. N. McAlinden, D. G. Glass, O. R. Millington, and A. J. Wright, "Designing an experiment to measure cellular interaction forces," Proceedings of SPIE, **8810**, 88101L (2013).
13. R. W. Bowman, G. Gibson, D. Carberry, L. Picco, M. Miles, and M. J. Padgett, "iTweezers: Optical micromanipulation controlled by an Apple iPad," J. Opt. **13**, 044002 (2011).
14. M. J. Padgett and R. Di Leonardo, "Holographic optical tweezers and their relevance to lab on chip devices," Lab Chip **11**, 1196–11205 (2011).
15. M. K. Cheezum, W. F. Walker, and W. H. Guilford, "Quantitative Comparison of Algorithms for Tracking Single Fluorescent Particles," Biophys. J. **81**(4), 2378–2388 (2001).
16. D. D. Udrea, P. J. Bryanston-Cross, W. K. Lee, and M. Funes-Gallanzi, "Two sub-pixel processing algorithms for high accuracy particle centre estimation in low seeding density particle image velocimetry," Opt. Laser Technol. **28**(5), 389–396 (1996).
17. M. V. Kristensen, P. Ahrendt, T. B. Lindballe, O. Højager Attermann Nielsen, A. P. Kylling, H. Karstoft, A. Imparato, L. Hosta-Rigau, B. Stadler, H. Stapelfeldt, and S. R. Keiding, "Motion analysis of optically trapped particles and cells using 2D Fourier analysis," Opt. Express **20**(3), 1953–1962 (2012).
18. J. Guck, R. Ananthakrishnan, H. Mahmood, T. J. Moon, C. C. Cunningham, and J. Käs, "The Optical Stretcher: A Novel Laser Tool to Micromanipulate Cells," Biophys. J. **81**(2), 767–784 (2001).
19. X. Wang, S. Chen, M. Kong, Z Wang, K. D. Costa, R. A. Li, and D. Sun, "Enhanced cell sorting and manipulation with combined optical tweezer and microfluidic chip technologies," Lab Chip **11**(21), 3656–3662 (2011).
20. N. McAlinden, D. G. Glass, O. Millington, and A. J. Wright, "Viability studies of optically trapped T-cells," Proceedings of SPIE, **8097**, 80970J (2011).
21. D. B. Phillips, S. H. Simpson, J. A. Grieve, G. M. Gibson, R. Bowman, M. J. Padgett, M. J. Miles, and D. M. Carberry, "Position clamping of optically trapped microscopic non-spherical probes," Opt. Express **19**(21), 20622–20627 (2011).

1. Introduction

Optical trapping (sometimes known as laser tweezers) is a well-established, well characterised technique that has been around for over thirty years and allows users to manipulate and control micron sized objects using a tightly focussed laser beam [1]. It has found application across the science disciplines and, in particular, is of growing demand in many fields of life science research. Many quantitative optical trapping experiments rely on manipulating beads that have been coupled to the target(s) of interest for the purpose of the experiment. Depending on the application, these beads can be coated with biologically-active molecules to instigate a response from a cellular sample. For example, several papers describe the use of optically trapped polystyrene beads coated with cell-activating antibodies and investigate their interaction with T cells [2–5] to assess the role of cell orientation upon activation [6] or to combine with calcium imaging [7].

The dynamics of an optically trapped bead can be likened to that of a thermally excited, damped harmonic oscillator, where the restoring force is generated by the highly focused laser beam and the damping force is provided by the surrounding medium [8]. For small displacements from equilibrium position, x, an optical trap can be modelled as a harmonic potential, $U(x)$, where $U(x) = \frac{1}{2}\kappa\langle x^2\rangle$ and the optical force, $F(x)$, can be described as a mass on a spring with $F(x) = -\kappa x$. κ is the spring constant or trap stiffness, often expressed in pN/nm, it is a measure of how strongly the object is trapped and is proportional to laser power. The trap stiffness can be calibrated using the theory of equipartition of energy and equating the potential

#200917 - $15.00 USD Received 20 Nov 2013; revised 20 Dec 2013; accepted 20 Dec 2013; published 3 Mar 2014

energy of the trap to the thermal energy given by $\frac{1}{2}K_BT$ where K_B is the Boltzmann constant and T the temperature, giving, $\kappa = K_BT/\langle x^2 \rangle$. Key to the majority force measurement experiments is accurate and reliable position sensing and particle tracking leading to the determination of the time-independent variance in the bead position $\langle x^2 \rangle$[9].

An optical trap works best for objects that are roughly spherical and 1-10 μm in diameter and it is therefore feasible to directly trap a cell of interest rather than an exogenous bead. For example, Andersson *et al*. optically trapped bone cells and used a viscous drag force method to calibrate the optical trapping force [10]. Alternatively, Oddos *et al*. directly trap T cells and antigen presenting cells to orientate the cell pair with respect to the imaging plane of their confocal microscope [11]. Problems arise when taking quantitative force measurements of the cell that involve observing and tracking the position of the trapped cell with time. Cells are never perfectly spherical and their refractive index is non-uniform leading to an inhomogeneous image when observed with a light microscope and causing issues for position sensing and particle tracking algorithms, many of which rely on a uniform image. In the case of large cells, an optical trap will often trap a single high refractive index feature of the cell (for example the cell nucleus) rather than the cell as a whole. This can lead to the cell re-orientating or rolling, making quantitative measurement difficult.

In this paper we first present a detailed study of the issues involved in accurately tracking the position of an optically trapped cell before discussing several approaches which can be taken to tackle these issues and ultimately allow the position of the cell to be reliably tracked. We show how designing a multi-point optical trap can allow the cell as a whole to be trapped, rather than just a single feature, removing issues associated with cell roll and re-orientation. We also present data tracking a fluorescently stained cell, which provides a more homogeneous image and enables more reliable tracking throughout an experiment. Our experimental data is supported with a detailed mathematical model highlighting the extent of the problem and the level of improvement that can be achieved using these techniques. In these studies we optically trap T cells, although the approaches presented could easily be adapted to suit a wide variety of cell types, including non-spherical cells. T cells and antigen presenting cells form part of the adaptive immune response system and how they interact with each other can inform vaccines and determine how the body fights a particular pathogen or disease. There is a growing interest in using optical tweezers in immunology and designing experiments to probe these interactions at a single cell level [11, 12]. Thus, methods to accurately track and control cell position and reorientation are essential and play a critical role in calibrating and quantifying optical traps.

2. Materials and methods

2.1. Experimental setup

Figure 1 shows the optical trapping set up. The beam from a continuous wave 3 W 1064 nm wavelength Laser (Ventus IR, Laser Quantum) is expanded to just overfill a Boulder Nonlinear Systems XY series Spatial Light Modulator (SLM). The SLM consists of 512×512 individually addressable pixels which alter the phase of the light. The SLM displays a hologram which is re-imaged onto the back aperture of the microscope objective using the relay optics shown in Fig. 1. Holograms are calculated and displayed on the SLM using the Red Tweezers software developed by the Optics Group at the University of Glasgow [13, 14]. Here we use the SLM to create 3 closely spaced traps, the positions of which can be individually selected so as to sit just inside the membrane of a particular cell/object of interest, creating a triple-spot trap and pinning the cell at 3 distinct positions. Example holograms for a single- and triple-spot trap are included in the insert in Fig. 1. Mirrors steer the laser beam into an inverted fluorescent microscope (Nikon TE2000-U). The objective used was a Nikon $\times 100$ oil immersion objective with a numerical aperture of 1.3. The beam size is matched to the back aperture of the objective to

#200917 - $15.00 USD Received 20 Nov 2013; revised 20 Dec 2013; accepted 20 Dec 2013; published 3 Mar 2014

ensure the largest possible electro-magnetic field gradient is achieved. With the laser operating at full power, the power at the sample was calculated to be 290 $\pm$ 5 mW, this was determined by placing the power meter before the objective and assuming 40% loses in the objective [8]. For these experiments the power at the sample was kept at 12 mW to prevent damaging the cells. The spot size is approximately diffraction limited with a diameter of $\sim$ 500 nm. The sample was imaged using a Dalsa Genie Camera, which could record images at a frame rate of up to 4 kHz with a limited region of interest (10 µm $\times$ 10 µm). A QCam colour camera from QImaging was used for fluorescence imaging. It could record images at a frame rate of up to 40 Hz with a 10 µm $\times$ 10 µm region of interest. In these experiments carboxyfluorescein diacetate, succinimidyl ester (CFSE) (Life Technologies, Paisley, UK) was used as a fluorophore, it has an excitation maximum at 494 nm and peak in emission of 521 nm. A quad band filter cube (Semrock, DA/FI/TR/Cy5-A-NTE) was used for fluorescence imaging. The laser, SLM and cameras were all controlled using a LabVIEW program written specifically for this system; this program also tracked the position of the cell using a centre of mass tracking algorithm or cross correlation tracking algorithm and saved the x, y coordinates as a function of time.

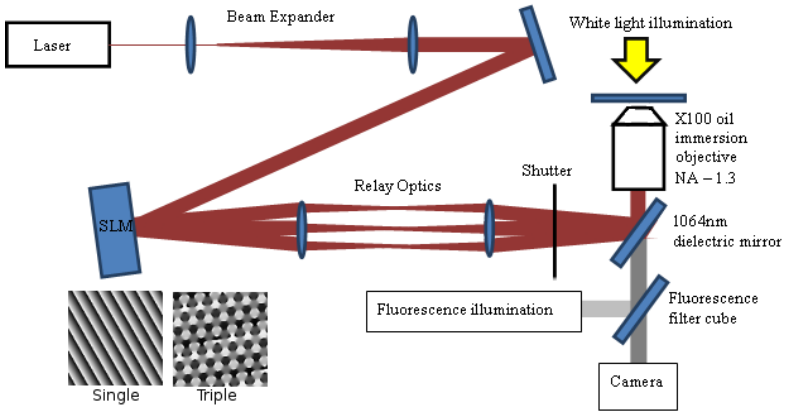

Fig. 1. Schematic of the experimental set up, including the laser, the Spatial Light Modulator (SLM), the oil immersion microscope objective, white light illumination, fluorescence illumination and camera. Also displayed is the hologram required for a single-spot trap (off set from the central position) and a triple-spot trap with 3 closely spaced traps, the grey scale representing a 0-2π phase change.

2.2. Tracking algorithms

A comprehensive review of the tracking algorithms used in optical tweezers and fluorescence microscopy can be found at [15]. Two algorithms in particular are used in this study and are discussed in this section.

2.2.1. Centre of mass tracking

Calculating the centre of mass of a greyscale image is computationally simple and fast and can be used to accurately calculate the distance an object has moved. The centre of mass along a single axis can be calculated using Eq. (1).

$$C_x = \sum_{i=1}^{m}\sum_{j=1}^{n}(x_i \mathbf{I}_{ij}) / \sum_{i=1}^{m}\sum_{j=1}^{n}\mathbf{I}_{ij} \tag{1}$$

#200917 - $15.00 USD Received 20 Nov 2013; revised 20 Dec 2013; accepted 20 Dec 2013; published 3 Mar 2014

where $\mathbf{I}_{ij}$ is a matrix of image pixel intensity. This algorithm works best for simple, circular, bright objects on a dark background, for this reason a threshold is often applied to the images to remove the background, creating a bright object on a dark background. Thresholding works well for optically trapped beads but it is not always easy to convert a white light transmission image of an inhomogeneous cell into a suitable image (see Fig. 2). The benefits of centre of mass tracking is speed and simplicity but it can produce mis-leading results when it comes to tracking non-uniform objects or objects that can rotate or change shape. This method has a tracking resolution less than the size of a camera pixel [15, 16].

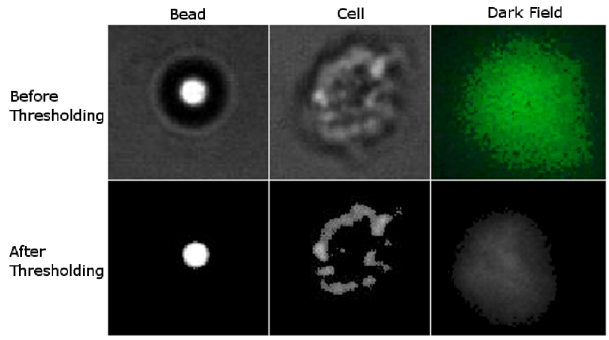

Fig. 2. Images of the different scenarios discussed here. The image of the bead is symmetric with large contrast between the centre and background making it simple to track. However, the contrast between the cell and background is poor and the cell is not symmetric. When the cell is flourescently stained and imaged in dark field the contrast and symmetry is improved.

2.2.2. Cross-correlation tracking

Cross-correlation is significantly more computational intensive than centre of mass tracking. It compares an image **I** to a reference image **K** and calculates the relative shift. It does this by moving the images over each other and calculating the point of most similarity. Eq. (2) calculates the cross correlation **X** of the two images **I** and **K**

$$\mathbf{X}_{x,y} = \sum_{i=0}^{m-1} \sum_{j=0}^{n-1} \mathbf{I}_{x+i,j+j} \left\{ \mathbf{K}_{i,j} \right\} \tag{2}$$

The centre of mass of the correlation image **X** gives the relative shift of the images. For cross-correlation to work successfully it is important to normalize the images since the algorithm will tend to match regions of highest intensity with each other. To speed up this calculation a fast Fourier transform method is normally used [17].

This method does not require thresholding to remove the background of the image and is much less susceptible to non-uniformities in the sample, object rotation or object changing shape. However, significant cell roll may cause problems and the maximum tracking rate will be reduced considerably when compared to centre of mass tracking. The cell drifting in and out of focus may also present problems for this algorithm.

2.3. Modelling the position of a trapped object

A simple model was developed to describe the motion of an object with non-uniform shape and refractive index, trapped in a single- and double-spot trap. The model developed followed a simple Brownian motion model but allowed the trapped object to exchange angular momentum

#200917 - $15.00 USD Received 20 Nov 2013; revised 20 Dec 2013; accepted 20 Dec 2013; published 3 Mar 2014

with the solvent (in this case water). To allow the model to calculate the motion of the object with reasonable speed on a desktop computer the model was a 2 dimensional representation of a trapped object. At each time point the cell was given a push from the solvent (Eq. (3)), this push had a random magnitude and direction and would act on a random point over the object's surface. Included in the model was the restoring force due to the trap (Eq. (4)) and a viscous drag force (Eq. (5)). The model assumed that the cell was not deformed by the viscous force. The forces required to deform a cell in an optical strecher are $\geq$ 10 times greater than the trapping forces in this model [18]. The pushing force can have components both parallel and perpendicular to a line between the cell surface where the force has acted and the trapping position. The parallel component will simply push the cell out of trap centre, with the trapping force restoring the cell to its central position. The perpendicular component will impart a torque on the cell and cause it to rotate. The angular acceleration of this rotation depends on the moment of inertia of the cell. To simplify the model the viscous drag force does not act to inhibit rotation so there is no restoring force included that will stop the cell rotating. The random force, $\vec{F_T}$, imparted on the solvent follows a normal distribution scaling with $k_B T$.

$$\left\langle \vec{F_T} \right\rangle = 0 \tag{3}$$

The restoring force due to the trap is given by,

$$\vec{F_R} = -\kappa \vec{x} \tag{4}$$

where κ is the spring constant of the trap. The viscous drag force is given by,

$$\vec{F_D} = 6\pi r \eta \frac{d\vec{x}}{dt} \tag{5}$$

where r is the radius of the cell η is the viscosity of the solvent.

When two or more traps are included the calculation is more difficult. At each time point the torque for each trap must be calculated and summed. If the cell has rotated due to the pushing force there will be a restoring torque due to one or the more of the traps no longer being in their zero position. This torque is calculated by first calculating the force from Eq. (4) and multiplying it by the radius of the cell.

At each time point the position of a point within the cell is recorded. This position does not have to be the centre of the cell or one of the trapping positions.

It should be noted that as the model was in 2 dimensions only two traps were required to eliminate cell roll as the cell cannot rotate out of the plane that is modelled. However, if a 3 dimensional system is studied 3 traps are required to prevent cell roll in all directions.

3. Results

3.1. Problems with trapping asymmetric objects

To understand the problems associated with trapping a non-uniform object (such as a cell) with a standard Gaussian beam, a sequence of images of a typical trapped cell were acquired and x-y position scatter plots and position versus time plots calculated (Fig. 3). Included in Fig. 3 are an equivalent set of results but taken with a trapped bead of a similar size to the cell for comparison. These clearly highlight the difficulties that occur when trying to accurately define cell position as opposed to the ease of homogeneous beads. A simple solution that can be used to help calculate the trap spring constant is to apply a smoothing algorithm to remove the large features associated with a cell roll, Fig. 3(d). This works as the cell roll is a much slower event than the Brownian motion that we are interested in. However, a small artefact

#200917 - $15.00 USD Received 20 Nov 2013; revised 20 Dec 2013; accepted 20 Dec 2013; published 3 Mar 2014

remains after smoothing which will still affect the accuracy of any calibration. While trapping a 6 μm spherical polymer bead with a single-spot optical trap, a $\sim$ 5 % error (Standard Deviation (SD)$\times$100/Trap Spring Constant (κ), N = 20 (each experiment involved recording 10,000 data points)) would be expected, this error will mostly be due to systematic errors such as, camera noise and system vibrations. However, when a cell is trapped with a single-spot trap this can be up to 35 % (SD$\times$100/κ, N = 20) due to cell roll. By using a 100 point floating average this error can be significantly reduced, to $\sim$15 % (SD$\times$100/κ, N = 20), but great care must be taken as the measured spring constant can depend strongly on the number of points chosen in the floating point average. In this case a 1000 floating point average gives a trap strength of 1.3 $\pm$ 0.6 pN/mm^2 , a 100 point average gives 1.2 $\pm$ 0.2 pN/mm^2 and a 25 point average gives 1.8 $\pm$ 0.1 pN/mm^2. Clearly the 25 point average has overestimated the spring constant. In the case of Fig. 3(c) there is also a significant error in measuring the cell surface position when the cell rolls. In the case of the bead there is an error in position of 0.07 μm while in the case of the cell this error is significantly larger 0.4 μm. If a cell needs to be positioned accurately to make contact with a surface or another cell this error could cause significant problems. It may also cause issues in cell sorting applications of optical trapping [19].

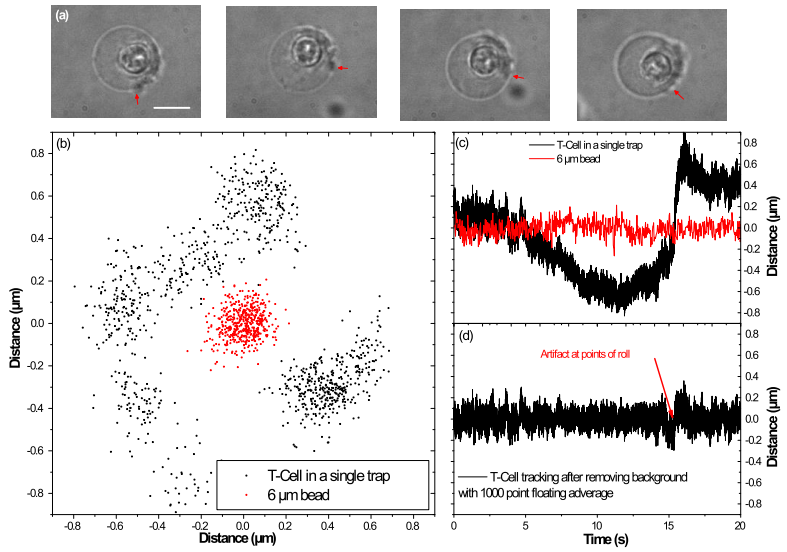

Fig. 3. (a) A series of white light transmission images showing a T-cell rotating in a single-spot trap as the microscope stage is moved. Red arrows are a guide for the eye highlighting the same spot on the cell in each image. The white bar represents 10 μm. (b) Scatter plots comparing the position determined by centre of mass tracking of an optically trapped bead (red) and cell (black) recorded over a 20 second time frame using a single-spot trap with the sample stage held stationary. A bead of similar size to the trapped cell was used. (c) The same data as (b) but looking at a single axis over time, the influence of cell roll on the data clearly visible. (d) By subtracting a 1000 point floating average from the cell position data presented in (c), the impact of cell roll has been greatly reduced but still visible as indicated by the arrow.

3.2. Multiple spot trap

The mathematical model described in section 2.3 was then used to ascertain if a novel trapping geometry would reduce the effect of cell roll and allow for an accurate measurement of the

#200917 - $15.00 USD Received 20 Nov 2013; revised 20 Dec 2013; accepted 20 Dec 2013; published 3 Mar 2014

optical trapping force. In Fig. 4 the model is used to determine the effect of trapping an inhomogeneous object with a double-spot trap as opposed to a single-spot trap. Figure 4(a) shows a scatter plot comparing the single- and double-spot trapping geometry. For the single-spot trap, the model aligns well with the experimental data presented in Fig. 3(b) and accurately represents the experimental situation. When a double-spot trap is used, the cell can no longer rotate. In Fig. 4(b) the position is plotted over time. In the case of the single-spot trap the influence of cell roll is clear. The mathematical model of the double-spot trap predicts that cell roll will be greatly reduced and that tracking of the inhomogeneous cell can become almost as accurate as experimental results achieved with an optically trapped bead (Fig. 3(c)). This effect was greatest when the two spots were as far apart as possible while remaining within the cell.

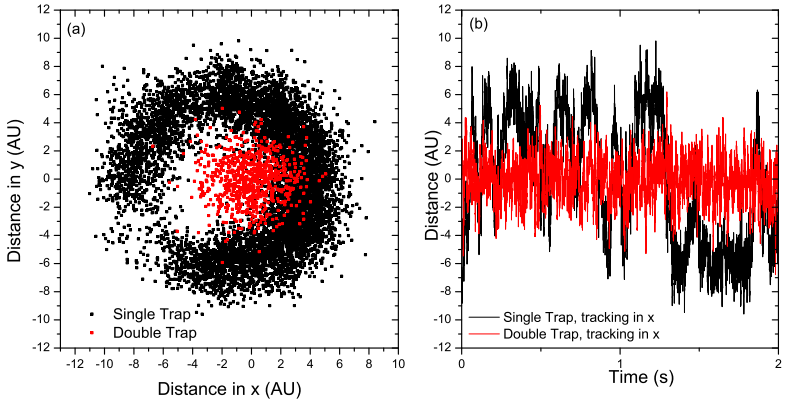

Fig. 4. (a) A scatter plot from a modelled single-(black) and double-spot trap (red). (b) Modelled position versus time data for a single- (red) and double-spot trap (black).

In Fig. 5 a T-cell is trapped with a triple-spot trap and compared with data that was achieved with a bead trapped using a standard single-spot trap and a cell trapped with a single-spot trap. From Fig. 5(a) it can be seen that the cell no longer rolls (compare to Fig. 3(a)) within the triple-spot trap as the microscope stage is moved. The power from the single-spot trap is distributed into the 3 individual traps which are placed near the edge of the cell equidistant from each other, resulting in a total trap stiffness that is the same as the single-spot trap stiffness. Figure 5(b) shows a scatter plot with the microscope stage held stationary, it is clear that the cell is no longer rotating/rolling and compares well to both a bead and the modelled data. The cell position and trap spring constant can be measured with a significantly higher accuracy as demonstrated with Fig. 5(c). The error in measuring the position of a cell trapped using a triple-spot trap is 0.05 μm in x and 0.06 μm in y comparing well to that of a bead trapped using a standard single-spot trap. This allows significantly more accurate control in positioning of cells. The error in trap spring constant for the cell is also greatly improved to $\sim$ 11 % (SD$\times$100/κ, N = 20).

3.3. Florescent imaging

The error in measuring cell position can be understood by looking at the images of a bead, cell and fluorescently stained cell (Fig. 2). In the case of the bead the image is a clear homogenous bright spot, this is made even clearer using a suitable thresholding. The centre of this object is easily calculated and can be accurately measured. In the case of the cell the contrast is not as high and finding a suitable threshold level is difficult. Even with thresholding the image is inhomogeneous and measurements of the centre of mass will clearly be susceptible to cell roll

#200917 - $15.00 USD Received 20 Nov 2013; revised 20 Dec 2013; accepted 20 Dec 2013; published 3 Mar 2014

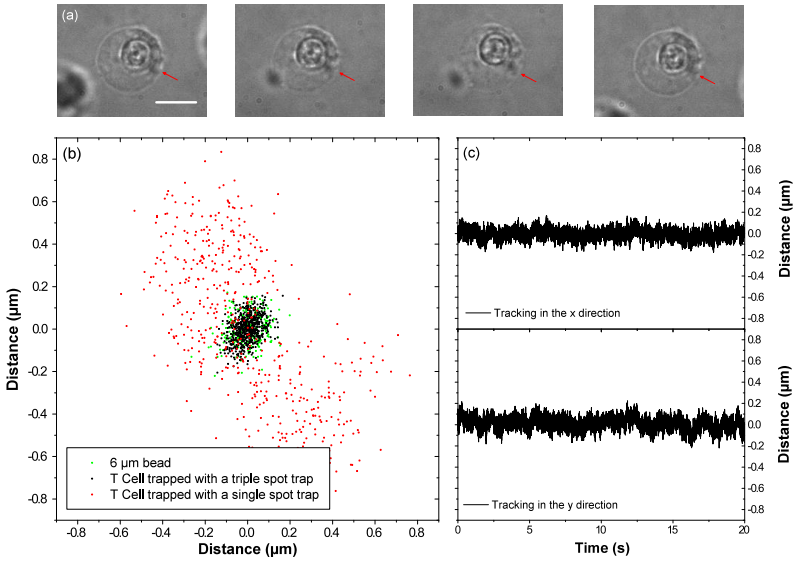

Fig. 5. (a) Sequence of images showing that a cell in a triple-spot trap does not rotate as the sample stage is moved. The white scale bar is 10 μm. The red arrow is a guide for the eye, indicating the same position on the cell in each image. (b) With the stage held stationary, a scatter plot of a cell trapped using a triple-spot trap (black) is compared that of a bead trapped using a single-spot trap (green) and a cell trapped using a single-spot trap. (c) The cell position versus time in both the x and y directions.

or the cell changing shape. When the cell is imaged in dark field fluorescence mode the contrast and homogeneity are both improved.

A second approach to improving the tracking of cells was to use a florescently stained cell, trapped with a standard single-spot trap, and tracked using centre of mass tracking, so that the cell would be free to roll but when imaged in dark field fluorescence it would appear uniform and hence would be easier to track. The cell was stained using a strong fluorophore (CFSE) and tracked and imaged in dark field mode using a centre of mass algorithm (Fig. 6). With the cell imaged in fluorescence, the tracking algorithm should follow the centre of the cell and not a bright feature on the periphery. Although this will not entirely remove the effects of cell roll, by tracking on the more homogenous fluorescence image it will ensure that it is the centre of the cell that is tracked, reducing the effects of any roll. Figure 6(a) shows a scatter plot from a CFSE stained cell in dark field mode trapped using a single-spot trap. Although the plot is similar to that of a bead of similar size there is still some structure related to cell roll. Figure 6(b) shows the position of the stained cell in x and y versus time. This method does not improve the calibration of cell position so does not help with applications where cell positioning is critical. However, it can improve the accuracy of calibrating the trap spring constant. The error in trap spring constant was found to be 13 % (SD$\times$100/κ, N = 10 (each experiment involves 500 data points)). Using this method the cell was tracked at a rate of 35 Hz. This compares to a rate of 1.1 kHz that was achieved with the bright field centre of mass tracking. There can also be problems associated with photobleaching using this method.

#200917 - $15.00 USD Received 20 Nov 2013; revised 20 Dec 2013; accepted 20 Dec 2013; published 3 Mar 2014

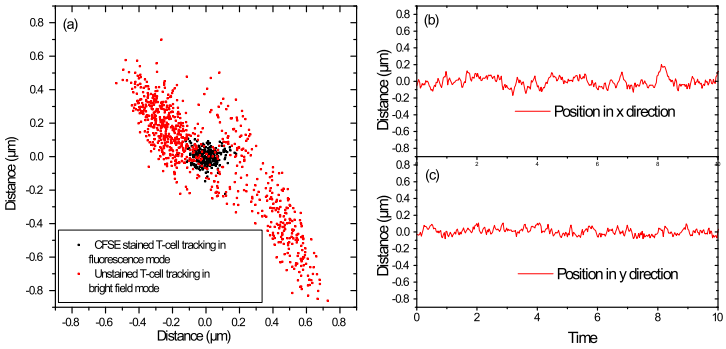

Fig. 6. (a) A scatter plot of a fluorescently stained cell trapped using a single-spot trap, imaged in dark field and tracked using the centre of mass tracking algorithm . The scatter plot is similar to that of a trapped bead of similar size and an un-stained cell trapped using a triple-spot trap. For comparison the scatter plot of an un-stained cell trapped with a single-spot trap in bright field mode is also shown. (b) The position of the fluorescently stained cell in x and y over time.

3.4. Cross correlation tracking

Finally an alternative tracking algorithm (cross correlation tracking [15–17]) was tested. Figure 7(a) and (b) show x, y scatter plots of a trapped cell for both a single- and triple-spot trap tracked using a cross correlation algorithm. This algorithm should be less susceptible to cell roll or the cell changing shape. However, significant cell roll will cause errors in tracking. It is clear that cell roll in the single-spot trap case (Fig. 7(a)) has caused problems for the tracking algorithm. The calibration error for the single-spot trap case was 19 % (SD$\times$100/κ, N = 20 (each experiment involves 1,000 data points)) suggesting that the algorithm had improved things slightly from the case of a single-spot trap tracking using a centre of mass algorithm. When the triple-spot trap was used the cell was held without rolling and was tracked accurately (Fig. 7(b)). This resulted in a calibration error or 10 % (SD$\times$100/κ, N = 20). This slight improvement in accuracy of calibration has come at a cost as the cell can only be tracked at a rate of $\sim$75 Hz using this algorithm.

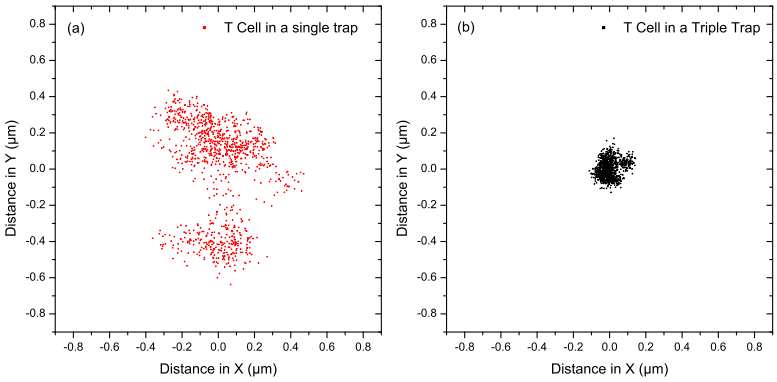

Fig. 7. Scatter plots of an optically trapped T cell, tracked using a cross correlation tracking algorithm, comparing a single-spot trap (a) to a triple-spot trap (b).

#200917 - $15.00 USD Received 20 Nov 2013; revised 20 Dec 2013; accepted 20 Dec 2013; published 3 Mar 2014

4. Discussion

Table 1 summaries the findings presented in the previous section, comparing the different strategies proposed to resolve the issues that arise when tracking the position of an optically trapped cell. The data achieved for a 6 μm diameter bead trapped with a single-spot trap and tracked using a centre of mass tracking algorithm is included as a bench mark and for comparison.

Table 1. Summary of results

Measurement Type	Frame Rate	Error (SD$\times$100/κ)	Positioning Error
Bead	1.1 kHz	5 %	0.07 μm
Single-spot Trap	1.1 kHz	35 %	0.4 μm
Floating Average	1.1 kHz	16 %	
Triple-spot Trap	1.1 kHz	11 %	0.055 μm
Florescence Cells	35 Hz	13 %	0.27 μm
Cross Correlation	75 Hz	19 %	0.21 μm

It is interesting to compare the triple-spot trap to the fluorescence imaging approach, the former looks to trap the cell as a whole and remove cell roll whereas in the later the cell is still free to roll and re-orientate but is imaged using fluorescence in dark field to produce an image closer to a bright spot on a dark background, an image more suitable for centre of mass tracking. The fluorescence imaging approach avoids miss-leading data points resulting from the algorithm incorrectly tracking a single high intensity feature of the image and instead tracks the average position of the cell with time. It is clear from table 1, that in terms of error in trap strength both improve the accuracy of the measurement with the triple-spot trap leading to the greater improvement.

In practice the choice of approach is likely to depend on the imaging and trapping system available. Not all optical trapping systems include a spatial light modulator to easily produce and position the three traps and similarly not all systems have a fluorescence imaging capability. Although, fluorescence is a common tool when working with cells and provides a useful functional read out of the system, it is however another artificial component being added to the system and is perhaps similar in this way to adding beads. There is of course no reason why a triple-spot trap and a fluorescence imaging approach cannot be combined and this could well be appropriate for some applications. The downside of any approach tracking a fluorescence image will always be the frame rate at which it is possible to image and the problem of photobleaching the sample during the measurement.

5. Conclusion

As the number of applications of optical trapping in the Life Sciences increases so does the need to perform accurate quantitative experiments that directly trap cells, removing the requirement for introducing exogenous beads. This poses a number of challenges when it comes to accurately tracking the position of the cell and reliably characterising and calibrating the optical trap. Cells are large compared to beads and have varying refractive indices and therefore are prone to roll and re-orientate rather than remain fixed in the trap. Here we have proposed several solutions to tackle this issue including a novel trapping geometry to trap the cell as a whole rather than a single feature of the cell, imaging in fluorescence in order produce an image closer to that of a bead and using a cross-correlation tracking algorithm. Fluorescent imaging and cross-correlation tracking were found to have significant negative impact when it came to the speed at which the cell could be tracked. It is common to determine the variance in position from several thousand readings and therefore a decrease in frame rate from 1.1 kHz to 35

#200917 - $15.00 USD Received 20 Nov 2013; revised 20 Dec 2013; accepted 20 Dec 2013; published 3 Mar 2014

Hz, when comparing fluorescence imaging to a centre of mass approach using the fast CMOS camera, greatly increases the timescales of the experiment.

Using a triple-spot trap to trap the cell as a whole gave the best all round result, reducing the error in k from 35% to 11% when compared to the single-spot trap and approaching an error of 5% in κ achieved when trapping a bead in a standard single-spot configuration. Demonstrating that we were able to fix the position of the cell and remove cell roll, allowing the standard fast camera and centre of mass tracking approaches to be used and hence giving a frame rate of 1.1 kHz. The position of the three traps can be altered easily using the red tweezers software making it suitable for a variety of cells of varying sizes. This approach would also be well suited to experiments where control over cell positioning is critical, for example cell sorting experiments. It has also been shown that by splitting the power of the laser beam between three trapping positions any cell photo-damage can be significantly reduced [20]. Further work may also include position clamping, which has been shown to be particularly useful when trapping non-spherical objects [21].

These findings are confirmed by a computational model used to describe the instabilities in the system and compare an inhomogeneous object trapped with a single-spot trap or a double-spot trap configuration, the two dimensional model with the double-spot trap being analogous to the triple-spot trap in practice. It is important to note that cell roll and re-orientation are not always a result of viscous drag forces or thermal currents but can occur spontaneously in a system due to Brownian motion.

Acknowledgments

This work was supported by the Engineering and Physical Sciences Research Council (AJW), the Royal Academy of Engineering via a Personal Research Fellowship (AJW) and an RCUK Fellowship (ORM).

#200917 - $15.00 USD Received 20 Nov 2013; revised 20 Dec 2013; accepted 20 Dec 2013; published 3 Mar 2014